MODELING OF SHEAR-YIELDING MEMBERS FOR SEISMIC ENERGY DISSIPATION

Afsin SARITAS[1] and Filip C. FILIPPOU[2]

SUMMARY

Structural members yielding in shear are used in earthquake resistant systems, such as eccentrically braced steel frames and systems with passive energy dissipation devices, in a conscious effort to concentrate the energy dissipation capacity of the structure in components that can be repaired or replaced after a major earthquake. The simulation of the energy dissipation capacity of these components is important in the evaluation of the seismic response of these structural systems. This paper presents a new beam element for the simulation of the hysteretic behavior of shear-yielding members. The element is based on a three-field variational formulation with independent force, displacement and deformation fields. The displacement field is based on Timoshenko's shear beam theory. The nonlinear response of the element arises from the integration of biaxial stress-strain relations over several control sections along the element length. The biaxial material model accounts for the interaction between normal and shear stress. While previous concentrated plasticity models involve parameter tuning for different loading and support conditions, the proposed model is general in its derivation of the axial force-shear-flexure interaction from the material response. The proposed model shows the characteristic advantages of force-based beam elements and is capable of simulating the inelastic response of short beams with a single element without suffering from shear locking. The effect of shear is significant in these members during the elastic and inelastic response. The ability of the model to accurately represent the hysteretic behavior of short shear-yielding members is ascertained with correlation studies of analytical results with available experimental data from shear-link experiments.

INTRODUCTION

Ductile yielding of members in shear represents an effective mechanism of energy dissipation in earthquake resistant structural systems. Short shear-yielding members appear first as shear-links of eccentrically braced frames (EBF) in the work by Roeder and Popov [1], Hjelmstad and Popov [2], and Kasai and Popov [3]. These studies led to the wide adoption of eccentrically braced frames in earthquake resistant design. The idea of utilizing shear yielding members as energy dissipation devices gave inspiration for the development of more recent innovative structural systems such as disposable knee braced frames by Balendra et al. [4], aluminum shear-links by Rai and Wallace [5], hybrid-coupled walls by Harries et al. [6], and proposal for structural rehabilitation by Ghobarah and Elfath [7]. More recently,

---
[1] Civil & Env. Engrg., Univ. of California, Berkeley, CA 94720, USA, E-mail: asaritas@ce.berkeley.edu
[2] Civil & Env. Engrg., Univ. of California, Berkeley CA 94720, USA, E-mail: filippou@ce.berkeley.edu

shear-links will be used as energy dissipation device between the tower shafts of the new San Francisco-Oakland Bay Bridge east span (McDaniel et al. [8]).

Modeling efforts for shear-yielding members to date center on relatively simplistic modifications of the one-component and two-component model Giberson [9]. In these models inelastic action is concentrated at the element ends in the form of elastic-perfectly plastic springs. Roeder and Popov [10], Ricles and Popov [11], and Ramadan and Ghobarah [12] have used variations of this general concept to arrive at a simple representation of the effect of shear on the plastic moment capacity of short steel members. These models suffer from two drawbacks: (a) they use available experimental data to derive conclusions about the interaction effects, which work well in some cases, but not in others; they are, therefore, empirical in nature, and (b) they are subject to the well-known calibration limitations of the one-component model about a midspan point of inflection in the member. This may not be accurate in long links under the combined effect of axial force, shear and bending moment. Models with such strong empirical basis and dependence of parameters on loading and boundary conditions lack generality and cannot be used in predictive studies of structural system response. To alleviate the lack of such a model the proposed beam element is based on distributed inelasticity in the member with integration of biaxial material response in several control sections. Even though it is clearly more complex than the previous models, it displays robust numerical behavior and is characterized by the ability to represent accurately the response of short and long shear-links over a wide range of loading conditions without the need of parameter calibration. It is this latter aspect that makes it useful in system response investigations of earthquake resistant structures with shear-yielding members.

FINITE ELEMENT FORMULATION

Beam element formulations based on displacement interpolation polynomials suffer from shear locking. To mitigate this problem several solutions have been proposed in the literature (Bathe [13]). The formulation in this paper eliminates the locking problem with the use of independent generalized stress, generalized strain, and displacement interpolation in a three-field Hu-Washizu functional, as described for the general case in Taylor et al. [14]. With $\boldsymbol{\sigma}$ denoting the stress tensor, $\boldsymbol{\varepsilon}$ the strain tensor, and $\mathbf{u}$ the displacements we have

$$\Pi_{\mathrm{HW}}(\boldsymbol{\sigma},\boldsymbol{\varepsilon},\mathbf{u}) = \int_{\Omega} W(\boldsymbol{\varepsilon})\,\mathrm{d}\Omega + \int_{\Omega} \boldsymbol{\sigma}^{\mathrm{T}}\left(\boldsymbol{\varepsilon}^{\mathbf{u}} - \boldsymbol{\varepsilon}\right)\mathrm{d}\Omega + \Pi_{\mathrm{ext}} \tag{1}$$

$W(\varepsilon)$ is the strain energy function, $\boldsymbol{\varepsilon}^{\mathbf{u}}$ denotes the strains derived from displacement compatibility, and Π_{ext} is the potential energy of the external loading due to body forces, displacement, and traction boundary conditions. In (1), the domain of the element is denoted by Ω, the traction boundaries are denoted by Γ_{t}, and the displacement boundaries by Γ_{u}.

Kinematic Approximations
Limiting ourselves to the planar case, we base the displacement field $\mathbf{u}$ in (1) on the assumptions of the Timoshenko beam theory

$$\mathbf{u} = \begin{bmatrix} u_{\mathrm{x}}(x,y) & u_{\mathrm{y}}(x,y) \end{bmatrix}^{\mathrm{T}} = \begin{bmatrix} u(x) - y\theta(x) & w(x) \end{bmatrix}^{\mathrm{T}} \tag{2}$$

where $u(x)$ is the axial displacement of the beam axis, $\theta(x)$ is the rotation of the beam cross section, and $w(x)$ is the transverse displacement of the beam axis.

The compatible strains for the displacement field in (2) result by appropriate differentiation

$$\varepsilon_{xx}^u = u'(x) - y\theta'(x) \quad \text{and} \quad \gamma_{xy}^u = -\theta(x) + w'(x) \tag{3}$$

The three-field variational form offers flexibility in selecting strain fields that are independent from the displacement compatible fields in (3). We denote these as follows

$$\varepsilon_{xx} = \varepsilon_a(x) - y\kappa(x) \quad \text{and} \quad \gamma_{xy} = \phi(y,z)\,\gamma(x) \tag{4}$$

$\varepsilon_a(x)$ is the axial deformation, $\kappa(x)$ is the curvature, and $\gamma(x)$ is the representative shear distortion along the beam axis. The variation of the shear strain field over the cross section is described by interpolation function $\phi(y,z)$. This function is derived by satisfying boundary conditions under elastostatic conditions with proper tractions on the surface of the beam. In this work, the simplification $\phi(y,z) \equiv \phi(y)$ is assumed, which is true for narrow beam sections or for problems where the Poisson effect is negligible.

Force Interpolation Functions
Taking the variation of the three-field functional in (1), and introducing the strain fields from (3) and (4) we obtain a reduced variational form. Integration by parts of all terms with derivatives in the displacement fields reveals the suitable interpolation functions for the section forces (generalized stress terms). Moreover this approach results in the elimination of the need for a displacement field approximation along the beam. A detailed presentation of the process is given in Taylor et al. [14]. For uniform member forces the force interpolation functions are

$$\mathbf{s}(x) = \mathbf{b}(x)\mathbf{q} + \mathbf{s}_p(x) \tag{5}$$

$\mathbf{s}(x) = \begin{bmatrix} N(x) & M(x) & V(x) \end{bmatrix}^T$ is the vector of section force resultants or generalized stresses, $\mathbf{q} = \begin{bmatrix} q_1 & q_2 & q_3 \end{bmatrix}^T$ represents the basic element forces (Figure 1), and $\mathbf{b}(x)$ is a matrix of force interpolation functions.
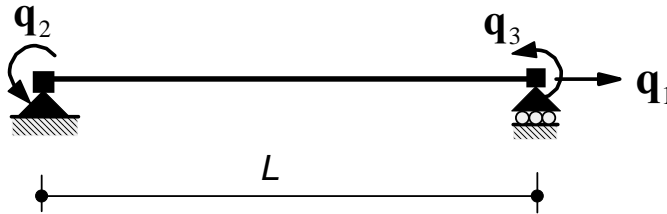

Figure 1: Basic forces and deformations of beam element

The matrix of force interpolation functions along with the section stress resultants $\mathbf{s}_p(x)$ due to element loading $\mathbf{w}$ is given by the following expressions

$$\mathbf{b}(x) = \begin{bmatrix} 1 & 0 & 0 \\ 0 & \dfrac{x}{L}-1 & \dfrac{x}{L} \\ 0 & -\dfrac{1}{L} & -\dfrac{1}{L} \end{bmatrix} \quad \text{and} \quad \mathbf{s}_p(x) = \begin{bmatrix} L\left(1-\dfrac{x}{L}\right) & 0 \\ 0 & \dfrac{1}{2}L^2\left[\left(\dfrac{x}{L}\right)^2 - \dfrac{x}{L}\right] \\ 0 & \dfrac{1}{2}L\left(1-2\dfrac{x}{L}\right) \end{bmatrix} \underbrace{\begin{pmatrix} w_x \\ w_y \end{pmatrix}}_{\mathbf{w}}$$ (6)

The following variational form is obtained after substitution of the preceding field variables,

$$\delta\Pi_{\mathrm{HW}} = \int_0^L \delta\mathbf{e}^{\mathrm{T}}\left[\hat{\mathbf{s}} - \mathbf{b}(x)\mathbf{q} - \mathbf{s}_p\right]dx - \delta\mathbf{q}^{\mathrm{T}}\int_0^L \mathbf{b}(x)^{\mathrm{T}}\mathbf{e}\,dx + \delta\mathbf{q}^{\mathrm{T}}\mathbf{a}\bar{\mathbf{u}} + \delta\bar{\mathbf{u}}^{\mathrm{T}}\mathbf{a}^{\mathrm{T}}\mathbf{q} - \delta\bar{\mathbf{u}}^{\mathrm{T}}\mathbf{p}_w$$ (7)

$\mathbf{e} = \begin{bmatrix} \varepsilon_a & \kappa & \bar{\gamma}(x) \end{bmatrix}^{\mathrm{T}}$ is the section deformation vector and $\mathbf{v} = \begin{bmatrix} v_1 & v_2 & v_3 \end{bmatrix}^{\mathrm{T}}$ is the element deformation vector. The element deformations can be obtained from the end displacements $\bar{\mathbf{u}}$ in the local reference system by the linear relation $\mathbf{v} = \mathbf{a}\bar{\mathbf{u}}$, where $\mathbf{a}$ is a simple transformation matrix for removing the rigid body modes from the end displacement vector under linear geometry. Details can be found elsewhere (Filippou and Fenves [15]). Finally, $\mathbf{p}_w = \begin{bmatrix} w_x L & w_y L/2 & 0 & 0 & w_y L/2 & 0 \end{bmatrix}^{\mathrm{T}}$ are the end forces due to element loads.

Final Form of the Element Formulation
The matrix expression of the variational form is obtained by evaluating the integrals in (7) at discrete integration points or control sections

$$\delta\Pi_{\mathrm{HW}} = \begin{bmatrix} \delta\bar{\mathbf{u}} \\ \delta\mathbf{q} \\ \delta\mathbf{e}_l \end{bmatrix}^{\mathrm{T}} \left\{ \begin{bmatrix} \mathbf{0} & \mathbf{a}^{\mathrm{T}} & \mathbf{0} \\ \mathbf{a} & \mathbf{0} & -\mathbf{b}(x_l)^{\mathrm{T}} \\ \mathbf{0} & -\mathbf{b}(x_l) & \mathbf{0} \end{bmatrix} \begin{bmatrix} \bar{\mathbf{u}} \\ \mathbf{q} \\ \mathbf{e}_l \end{bmatrix} - \begin{bmatrix} \mathbf{p}_w \\ \mathbf{0} \\ \mathbf{s}_{p,l} - \hat{\mathbf{s}}_l \end{bmatrix} \right\} = 0$$ (8)

where l denotes the integration point.

Due to the nonlinear nature of the problem, (8) is linearized relative to a reference point,

$$\begin{bmatrix} \mathbf{0} & \mathbf{a}^{\mathrm{T}} & \mathbf{0} \\ \mathbf{a} & \mathbf{0} & -\mathbf{b}(x_l)^{\mathrm{T}} \\ \mathbf{0} & -\mathbf{b}(x_l) & \mathbf{k}_{s,l} \end{bmatrix} \begin{bmatrix} \Delta\bar{\mathbf{u}} \\ \Delta\mathbf{q} \\ \Delta\mathbf{e}_l \end{bmatrix} = \begin{bmatrix} \mathbf{p}_w - \mathbf{a}^{\mathrm{T}}\mathbf{q} \\ -\mathbf{a}\bar{\mathbf{u}} + \mathbf{b}(x_l)^{\mathrm{T}}\mathbf{e}_l \\ \mathbf{b}(x_l)\mathbf{q} + \mathbf{s}_{p,l} - \hat{\mathbf{s}}_l \end{bmatrix}$$ (9)

The section tangent stiffness for integration point l is $\mathbf{k}_{s,l} = \partial\hat{\mathbf{s}}_l/\partial\mathbf{e}_l$.

The section deformations $\mathbf{e}_l$ and basic element forces $\mathbf{q}$ can be condensed out at the element level in (9) resulting in a modified stiffness expression for the element with mixed formulation. With this approach the element end displacement-end force relation is obtained in a form such that the element can be directly implemented in commonly available finite element platforms that make use of the direct stiffness implementation of the displacement method of analysis. The implementation of the element is discussed by Taylor et al. [14].

Section Modeling

Shear-link members have regular symmetric cross sections. Most common are wide flange sections, but rectangular sections are also used in energy dissipation devices. In either case the section deforms in-plane. On account of the symmetry of the cross section shear forces do not give rise to torsional moments either and torsional effects are minimal. The section deformations can be expressed in accordance with the relations in (4), which can be written in compact form as

$$\boldsymbol{\varepsilon} = \mathbf{a}_s \mathbf{e}, \quad \text{where} \quad \mathbf{a}_s = \mathbf{a}_s(y,z) = \begin{bmatrix} 1 & -y & 0 \\ 0 & 0 & \psi(y) \end{bmatrix} \tag{10}$$

The shear strain distribution function $\psi(y) = \varphi(y)/\beta$ depends on an assumption about function $\varphi(y)$ and on the scale parameter β. The parameter is selected so that the shear strain energy of the cross section with strain distribution $\psi(y)$ is equal to the shear strain energy under a constant strain value that is equal to the maximum value of $\psi(y)$. With this scaling there is no need for a shear correction factor.

Section forces derived from the section deformations and the corresponding section tangent stiffness matrix can be obtained from the following expressions

$$\hat{\mathbf{s}} = \begin{bmatrix} \hat{N} & \hat{M} & \hat{V} \end{bmatrix}^{\mathrm{T}} = \int_A \mathbf{a}_s^{\mathrm{T}} \hat{\boldsymbol{\sigma}}(\boldsymbol{\varepsilon}) \, dA \quad \text{and} \quad \mathbf{k}_s = \frac{\partial \hat{\mathbf{s}}}{\partial \mathbf{e}} = \int_A \mathbf{a}_s^{\mathrm{T}}(y) \mathbf{k}_m \mathbf{a}_s(y) \, dA \tag{11}$$

$\hat{\boldsymbol{\sigma}} = \begin{bmatrix} \sigma_{xx} & \sigma_{xy} \end{bmatrix}^{\mathrm{T}}$ and $\mathbf{k}_m$ is the material tangent stiffness $\mathbf{k}_m = d\hat{\boldsymbol{\sigma}}/d\boldsymbol{\varepsilon}$.

For a wide flange section a parabolic distribution is assumed for the shear strains and the resulting scale factor is

$$\psi(y) = \frac{1}{\beta}\left((1+2\alpha) - 4\frac{y^2}{d^2} \right) \quad \text{where} \quad \beta = \left((1+2\alpha)^2 - \frac{2}{3}(1+2\alpha) + \frac{1}{5} \right) \Big/ \left(\frac{2}{3}(1+3\alpha) \right) \tag{12}$$

where α is the ratio of the flange to the web area. For a rectangular section $\alpha = 0$ and the relation for the shear strain distribution simplifies to $5/4\left(1 - 4\,y^2/d^2\right)$. A similar approach was first proposed by Petrangeli et al. [16] in a model of the effect of shear on the hysteretic behavior of a reinforced concrete (RC) section. The model was developed in the context of a force-based beam element with layer discretization of the cross section. In the study both constant and variable shear strains were used for a rectangular RC section, with the conclusion that the shear strain profile should follow the distribution $3/2\left(1 - 4\,y^2/d^2\right)$.

Material Modeling

The accurate description of the hysteretic behavior of steel members by the proposed model depends on the representation of the material response. Even though a J_2 plasticity model is common in finite element analysis for the purpose, such a model is unable to represent accurately the hysteretic behavior of steel over several cycles of inelastic deformation. This fact is supported by the experimental observations of the shear link response for the specimens tested by Hjelmstad and Popov [2] and Kasai and Popov [3]. The following points are relevant: (a) cycling under constant inelastic deformation does not result in strength increase, (b) equal strength is observed under positive, or negative displacement values of equal magnitude, and, (c) a strength increase results when deformations exceed the values experienced during preceding cycles. Such hardening behavior cannot be obtained with the linear isotropic and kinematic hardening definitions of classical plasticity theory. This was confirmed by numerical simulations with a J_2 plasticity model that was calibrated to match the monotonic stress-strain behavior of the material. When

this model was cycled to the strain values measured in the tests, it exhibited excessive hardening.

To address the J_2 plasticity material model limitations, the generalized J_2 plasticity material model proposed by Lubliner et al. [17] was selected. This model is characterized by its simplicity and computational efficiency relative to nonlinear hardening and bounding surface plasticity models. In generalized plasticity theory, the inelastic response is governed by two functions: the limit function and the yield function, which is also present in classical plasticity theory. The limit function separates admissible from inadmissible stress states providing a smooth asymptotic transition between the elastic and inelastic state during loading of the material. This smooth transition is essential in approximating the Bauschinger effect under cyclic loading conditions. Under incomplete load reversal without change of sign for the stress, renewed plastic strain takes place before the material reaches the stress from which unloading initiated. The generalized plasticity model makes use of two additional parameters relative to classical J_2 plasticity theory: a parameter φ that measures the distance between the asymptotic yield surface and the current yield function, and a parameter δ that controls the curvature of the transition from the yield function to the asymptotic yield surface.

To establish a rational material description the parameters of the generalized J_2 plasticity model were calibrated by comparison of the material response with the extensive experimental measurements of cyclic uniaxial steel response by Panthaki [18]. The following model properties were found to exhibit good agreement with the experimental results: initial modulus $E = E_s$, isotropic hardening modulus $H_i \approx 0.0002E$, kinematic hardening modulus $H_k \approx 0.004E$, radius of yield function $\sigma_y \approx 0.85 f_y$, distance from asymptotic yield surface to yield function $\phi \approx f_u - f_y$, Poisson ratio $\nu = 0.3$, and transition parameter from yield function to asymptotic yield surface $\delta \approx 0.015E$. It can be observed that the isotropic hardening value is very small, while kinematic hardening is about 20 times higher, but still relatively small. With the above parameter selection the only free material parameters are the values of the initial elastic modulus E_s, the uniaxial yield strength f_y, and the uniaxial tensile strength f_u, which are readily available from the experimental data.

The generalized plasticity model by Lubliner et al. [17] is three dimensional, while the proposed beam element depends on only two stress values, the normal and shear stress at a material point of the cross section. For this case an algorithm similar to that proposed by Klinkel and Govindjee [19] is used to impose the condition of zero out-of-plane stress in the three dimensional constitutive model.

CORRELATION STUDIES

Specimen tested by Hjelmstad and Popov [2]
Hjelmstad and Popov [2] performed fifteen tests on full size shear-links to determine the general response of these short beams to cyclic loading. They have especially investigated the amount of web-stiffeners needed to prevent web buckling in order for the member to exhibit stable cyclic loops with significant energy dissipation. Their specimens were all tested under equal end moments at member ends. In the following figures we compare the analytical results with the measured response from specimen 4 of the Hjelmstad/Popov shear-link experiments. The geometric properties of the beam are shown in Figure 2. The beam cross section is a W18x40, the length L of the beam is 28 inches, and the depth d is 17.88 in, resulting in a span to depth ratio L/d of 1.56; the flange width b_f is 5.985 in, the web thickness t_w is 0.314 in, and the flange thickness t_f is 0.521 in. The plastic modulus about the major axis Z_x is 78.4 in^3.

For the analytical studies the link was represented by a single element with 3 Gauss-Lobatto integration points (control sections) along the span. Each section was subdivided into 16 layers, with four layers in

each flange and eight in the web. Midpoint evaluation of the distribution functions over the section was used. In the material description of the hysteretic behavior of each layer the following material properties were used (Hjelmstad and Popov [2]) : $E = 28000\,\text{ksi}$, $f_y = 35\,\text{ksi}$ and $f_u = 65\,\text{ksi}$. With these material properties the parameters of the generalized J_2 plasticity model are: Poisson ratio $\nu = 0.3$, isotropic hardening modulus $H_i = 5\,\text{ksi}$, kinematic hardening modulus $H_k = 112\,\text{ksi}$, distance of asymptotic yield surface from yield function $\phi = 30\,\text{ksi}$, and transition parameter $\delta = 420\,\text{ksi}$.

The shear links were tested with imposed end displacements at the right end, as shown in Figure 2.
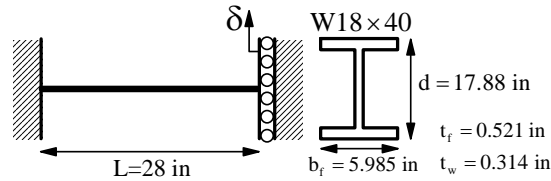
Figure 2: Specimen 4 - Hjelmstad and Popov [2]
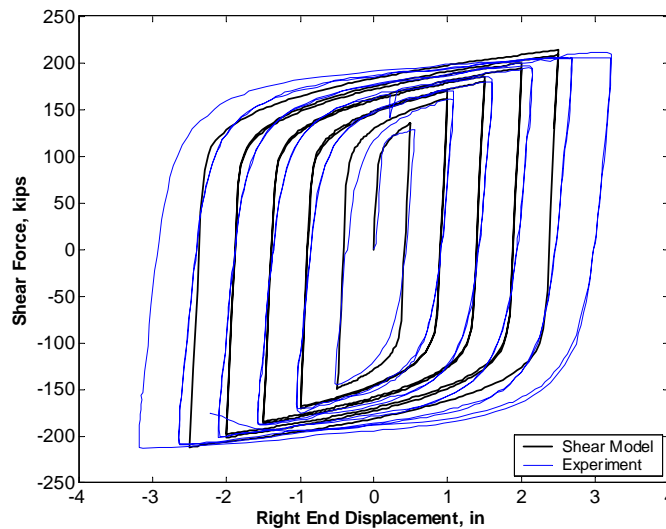
Figure 3: Analytical results vs. experimental data for specimen 4 by Hjelmstad and Popov [2]

The comparison of analytical results with experimental measurements of the hysteretic response of the shear-link specimen 4 are shown in Figure 3. Excellent agreement regarding strength and energy dissipation capacity is observed. A slight discrepancy in the unloading stiffness can be attributed to the observation in the original study that complete restraint of the rather short and, consequently, stiff specimen was not possible and that some slip of the specimen relative to the support was observed (Hjelmstad and Popov [2]). It is worth stressing that the excellent agreement is obtained with consistent material parameters with no additional adjustment. Thus, the results can be considered of predictive quality and confirm the rationality of the proposed model.

Specimen Tested by Kasai and Popov [3]
Kasai and Popov [3] performed seven tests for studying the effect of unequal end moments at the ends of the shear-link. When a shear-link is located next to a column in an eccentrically braced frame, the

moment at the column end of the link is generally much larger than the moment at the opposite end of the link. In order to induce such a moment distribution in the shear-link specimen, Kasai and Popov [3] selected the experimental set-up in Figure 4: at the end denoted with A the shear link is fully restrained; at the opposite shear-link end denoted with B, the shear link is connected to a beam segment with the same cross-section. The far end of the beam segment denoted with C in the figure is free. Two equal displacements are imposed at points B and C, so as to create a bending moment distribution with unequal end moments in the shear link.
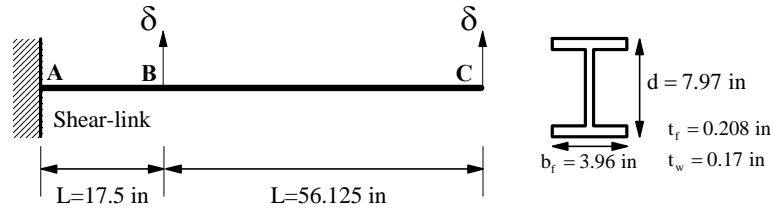
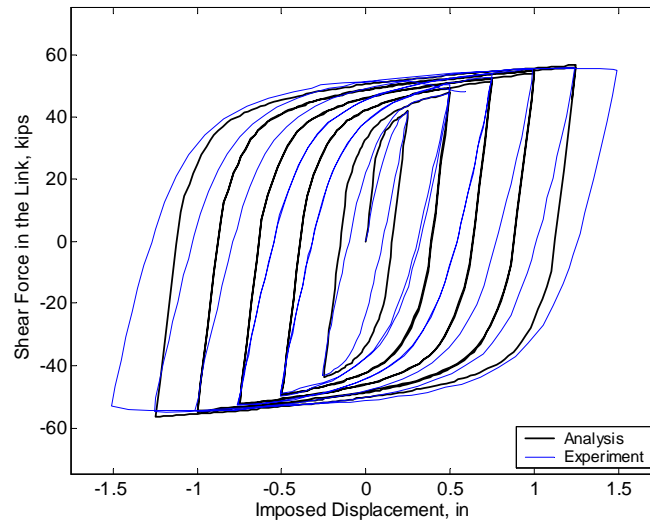

Figure 4: Specimen 5 from Kasai and Popov [3]

Figure 5: Analytical results vs. experimental data for specimen 5 by Kasai and Popov [3]

In the following correlation study specimen 5 from the Kasai and Popov [3] experiments is selected. The geometric properties of the specimen are listed in Figure 4. The long shear link has an aspect ratio L/d of 2.2. Its web is stiffened to ensure stable hysteretic behavior and delay local buckling. For the analytical studies the link was represented by a single element with 3 Gauss-Lobatto integration points (control sections) along the span. Each section was subdivided into 16 layers, with four layers in each flange and eight in the web. Midpoint evaluation of the distribution functions over the section was used. In the material description of the hysteretic behavior of each layer the following material properties were used (Kasai and Popov [3]) : $E = 29000\,\text{ksi}$, $f_y = 50\,\text{ksi}$ and $f_u = 70\,\text{ksi}$. With these material properties the parameters of the generalized J_2 plasticity model are: Poisson ratio $\nu = 0.3$, isotropic hardening modulus $H_i = 6\,\text{ksi}$, kinematic hardening modulus $H_k = 120\,\text{ksi}$, distance of asymptotic yield surface from yield function $\phi = 20\,\text{ksi}$, and transition parameter $\delta = 450\,\text{ksi}$.
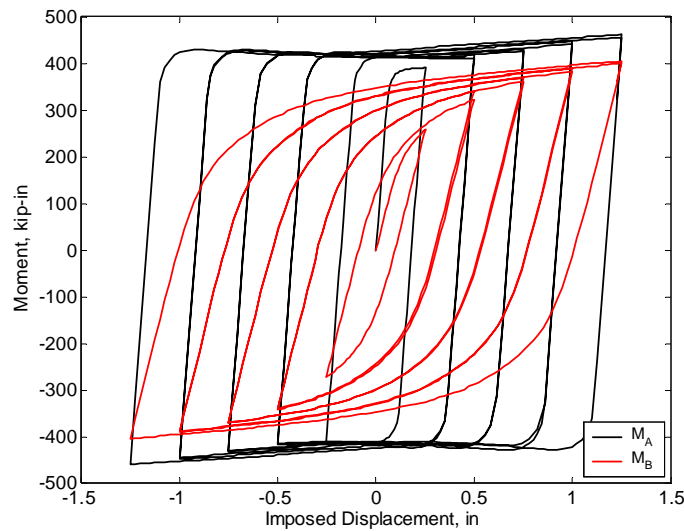
Figure 6: Analytical bending moment-displacement history at ends A and B
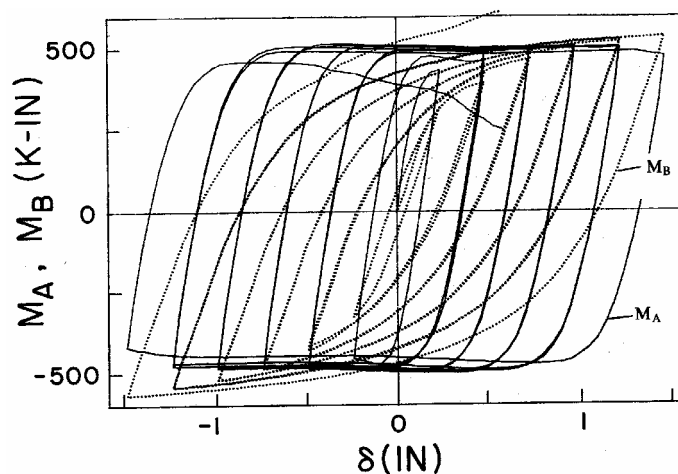

Figure 7: Measured moment-end displacement history for specimen 5 by Kasai and Popov [3]

The comparison of analytical results with experimental measurements of the hysteretic response of the shear-link specimen 5 are shown in Figure 5. Excellent agreement regarding strength and energy dissipation capacity for the entire shear link is observed in the shear-displacement relation of Figure 5. The comparison of analytical with experimental results for the end moment-displacement relation at ends A and B of the shear link can be established from Figures 6 and 7. While relatively good overall agreement is observed, the history of the relative moment values at the ends of the shear link is only approximated by the model. A similar observation was made in an earlier study by Ricles and Popov [20]. This is probably due to fact that the specimen suffered local buckling of the web and flange at end A, as corroborated by the negative slope of the moment-displacement relation as well as by the slight strength reduction in the later loading stages of Figure 7. This effect is not accounted for in the proposed section model. In spite of the presence of local buckling at end A, the specimen shows significant strength increase through strain hardening at end B. This is not captured by the model. We suspect that a complex three-dimensional behavior of the shear link is at the root of this phenomenon, on account of the interaction of the specimen with the loading device that maintains the displacement at end B equal to the

imposed displacement at the free end of the beam segment at point C in Figure 4. In any case, a more thorough analysis of the analytical results and comparison with three dimensional finite element models is planned in the future in order to understand better this phenomenon.

CONCLUSIONS

The proposed beam element that includes the interaction of axial force, bending moment and shear force is able to simulate accurately the hysteretic behavior of short and moderately long shear link in eccentrically braced frames or passive energy dissipation devices. It is noteworthy that analytical results of excellent accuracy were obtained with a consistent set of parameters for a generalized J_2 plasticity material model. These were derived by calibrating the model with uniaxial cyclic steel tests that were completely independent of the shear link specimens used in the correlation studies. The only material parameters for each investigation are the initial elastic modulus, the yield strength, and the ultimate tensile strength. These are readily available from coupon tests of the material. It is, therefore, possible to use the proposed model in a predictive setting for the analysis of structural elements and systems that employ shear elements for passive energy dissipation in earthquake resistant design.

REFERENCES

1.   Roeder, C.W. and E.P. Popov, *Eccentrically Braced Steel Frames for Earthquakes.* Journal of the Structural Division-ASCE, 1978. **104**(3): p. 391-412.
2.   Hjelmstad, K.D. and E.P. Popov, *Cyclic Behavior and Design of Link Beams.* Journal of Structural Engineering-ASCE, 1983. **109**(10): p. 2387-2403.
3.   Kasai, K. and E.P. Popov, *General Behavior of Wf Steel Shear Link Beams.* Journal of Structural Engineering-ASCE, 1986. **112**(2): p. 362-382.
4.   Balendra, T., M.T. Sam, C.Y. Liaw, and S.L. Lee, *Preliminary Studies into the Behavior of Knee Braced Frames Subject to Seismic Loading.* Engineering Structures, 1991. **13**(1): p. 67-74.
5.   Rai, D.C. and B.J. Wallace, *Aluminium shear-links for enhanced seismic resistance.* Earthquake Engineering & Structural Dynamics, 1998. **27**(4): p. 315-342.
6.   Harries, K.A., D. Mitchell, W.D. Cook, and R.G. Redwood, *Seismic Response of Steel Beams Coupling Concrete Walls.* Journal of Structural Engineering-ASCE, 1993. **119**(12): p. 3611-3629.
7.   Ghobarah, A. and H.A. Elfath, *Rehabilitation of a reinforced concrete frame using eccentric steel bracing.* Engineering Structures, 2001. **23**(7): p. 745-755.
8.   McDaniel, C.C., C.M. Uang, and F. Seible, *Cyclic testing of built-up steel shear links for the new bay bridge.* Journal of Structural Engineering-ASCE, 2003. **129**(6): p. 801-809.
9.   Giberson, M.F., *Two Nonlinear Beams with Definitions of Ductility.* Journal of the Structural Division, ASCE, 1969. **95**(ST2): p. 137-157.
10.   Roeder, C.W. and E.P. Popov, *Inelastic Behavior of Eccentric Braced Frames*. 1977, Earthquake Engineering Research Center, University of California, Berkeley.
11.   Ricles, J.M. and E.P. Popov, *Dynamic Analysis of Seismically Resistant Eccentrically Braced Frames*. 1987, Earthquake Engineering Research Center, University of California, Berkeley.
12.   Ramadan, T. and A. Ghobarah, *Analytical Model for Shear-Link Behavior.* Journal of Structural Engineering-ASCE, 1995. **121**(11): p. 1574-1580.
13.   Bathe, K.J., *Finite element procedures*. 1996, Englewood Cliffs: Prentice Hall.
14.   Taylor, R.L., F.C. Filippou, A. Saritas, and F. Auricchio, *Mixed finite element method for beam and frame problems.* Computational Mechanics, 2003. **31**(1-2): p. 192-203.
15.   Filippou, F.C. and G.L. Fenves, *Methods of Analysis for Earthquake-Resistant Structures*, in *Earthquake Engineering: From Engineering Seismology to Performance-Based Engineering*, Y. Bozorgnia and V.V. Bertero, Editors. 2004, CRC Press.

16.   Petrangeli, M., P.E. Pinto, and V. Ciampi, *Fiber element for cyclic bending and shear of RC structures. I: Theory.* Journal of Engineering Mechanics, ASCE, 1999. **125**(9): p. 994-1001.
17.   Lubliner, J., R.L. Taylor, and F. Auricchio, *A New Model of Generalized Plasticity and Its Numerical Implementation.* International Journal of Solids and Structures, 1993. **30**(22): p. 3171-3184.
18.   Panthaki, F.D., *Low Cycle Fatigue Behavior of High Strength and Ordinary Reinforcing Steels*, in *Department of Civil Engineering*. 1991, State University of New York: Buffalo, N.Y.
19.   Klinkel, S. and S. Govindjee, *Using finite strain 3D-material models in beam and shell elements.* Engineering Computations, 2002. **19**(7-8): p. 902-921.
20.   Ricles, J.M. and E.P. Popov, *Inelastic Link Element for EBF Seismic Analysis.* Journal of Structural Engineering, ASCE, 1994. **120**(2): p. 441-463.